Nuclear Engineering and Design 262 (2013) 264–275

Contents lists available at SciVerse ScienceDirect

Nuclear Engineering and Design

journal homepage: www.elsevier.com/locate/nucengdes

High fidelity simulation of conventional and innovative LWR with the coupled Monte-Carlo thermal-hydraulic system MCNP-SUBCHANFLOW

A. Ivanov[a,*], V. Sanchez[a], R. Stieglitz[a], K. Ivanov[b]

[a] Karlsruhe Institute of Technology, Institute of Neutron Physics and Reactor Technology, Herman-vom-Helmholtz-Platz-1, 76344 Eggenstein-Leopoldshafen, Germany
[b] The Pennsylvania State University, Department of Mechanical and Nuclear Engineering 206 Reber, University Park, PA 16802, United States

HIGHLIGHTS

- Coupled scheme between MCNP and in-house developed sub-channel code.
- We discuss the temperature dependence of nuclear data.
- We test the validity of the pseudo material mixing for thermal scattering data.
- The correlation between statistical uncertainty and convergence is investigated.
- The coupled scheme was applied to PWR, BWR and High Conversion PWR problems.

ARTICLE INFO

Article history:
Received 19 June 2012
Received in revised form 4 May 2013
Accepted 9 May 2013

Keywords:
Coupled codes
MCNP5
SUBCHANFLOW
Design
Safety
HPC

ABSTRACT

In order to increase the accuracy and the degree of spatial and energy resolution of core design studies, coupled 3D neutronic (multi-group deterministic and continuous energy Monte-Carlo) and 3D thermal-hydraulic (CFD and sub-channel) codes are being developed worldwide. At KIT, both deterministic and Monte-Carlo codes were coupled with sub-channel codes and applied to predict the safety-related design parameters such as critical power ratio, maximal cladding, fuel temperature and DNB. These coupling approaches were revised and improved based on the experience gained. One particular example is replacing COBRA-TF with SUBCHANFLOW, an in-house developed sub-channel code, in the COBRA-TF/MCNP coupling, accompanied with new way of radial mapping between the neutronic and thermal-hydraulic domains. The new coupled system MCNP5/SUBCHANFLOW makes it possible to investigate a variety of fuel assembly types. Key issues in such a coupled system are the implementation of the thermal-hydraulic/neutronic feedback mechanisms, the precision of the Monte-Carlo solutions, and the supervision of convergence during the iterative solution process. Another key issue considered is the optimal application of parallel computing. Using multi-processor computer architectures, it is possible to reduce the Monte-Carlo running time and obtain converged results within reasonable time limit. In particular, it is shown that by exploiting the capabilities of multi-processor calculation, large fuel assemblies on a pin-by-pin basis with a resolution at sub-channel level can be analyzed. One of the most important issues addressed in the current work is the temperature effects on nuclear data. For the particular studies pseudo material mixing approach was used to account for the temperature dependence of the nuclear data.

1. Introduction

High fidelity coupled solutions of neutron physics and thermal-hydraulic codes are being developed worldwide to increase the accuracy and the degree of spatial resolution of core design studies. For example coupled, Three-Dimensional (3D) neutronic (multi-group deterministic and continuous energy Monte-Carlo) and 3D thermal-hydraulic (CFD and sub-channel) codes were realized (Tippayakul et al., 2007; Watta et al., 2006; Puente Espel et al., 2009; Puente-Espel et al., 2010; Hoogenboom et al., 2011). At the Karlsruhe Institute of Technology (KIT), both deterministic and Monte-Carlo codes have been coupled with sub-channel codes and applied to predict the safety-related design parameters such as pin power, maximum cladding and fuel temperature of a PWR fuel assembly at nominal conditions (Sánchez et al., 2008; Sanchez and Al-Hamry, 2009).

The research done on the topic however, is mainly limited to small problems consisting of only few pins. For such problems the stability of the coupled system is not effectively tested. In the case

* Corresponding author.
E-mail addresses: aleksandar.ivanov@kit.edu (A. Ivanov), victor.sanchez@kit.edu (V. Sanchez), robert.stieglitz@kit.edu (R. Stieglitz), kni1@psu.edu (K. Ivanov).

0029-5493/$ – see front matter © 2013 Elsevier B.V. All rights reserved.
http://dx.doi.org/10.1016/j.nucengdes.2013.05.008

of large problems consisting of many thousands of cells, achieving convergence of the coupled calculation, convergence of the fission source and proper statistics poses a real challenge. Moreover, in the existing coupled systems classical thermal spectrum reactor geometries were considered (square BWR and PWR lattices). The main application of such a coupling system is to serve as numerical benchmark and to validate deterministic systems, especially innovative tight pitch hexagonal geometries, where the homogenization theory requires reliable validation. Therefore, having this in mind one requires the ability to model large problems within a consistent coupled system.

In the current paper, the further development and improvement of the existing coupling approaches will be presented. In particular, the COBRA-TF code was replaced by the in-house developed code SUBCHANFLOW, in the already existing COBRA-TF-MCNP5 coupled code system (Sanchez and Al-Hamry, 2009). In addition, a more generic radial mapping between the neutronic and the thermal-hydraulic domains was realized and new data interchanging subroutines were implemented. Those data interchange subroutines are able to create the complex geometry from simple input. The resulting MCNP input files easily exceed 200 thousand lines. The newly developed system MCNP5-SUBCHANFLOW makes it possible to investigate different types of fuel assemblies (BWR, PWR, High Conversion PWR (HCPWR)) without modifying the interface, used to exchange data between the thermal-hydraulic and the neutronic domains. Details of the coupling scheme, as well as the treatment of the temperature dependency of the continuous energy cross sections, via pseudo material mixing, will be presented in this paper. An extension of the pseudo material mixing methodology to thermal scattering data will also be presented. The application of the pseudo material mixing to both continuous energy and thermal scattering data is validated with respect to reference values, by comparing the k_∞.

Due to the statistical nature of MCNP and the requirement to simulate large number of particles, in order to obtain tally estimates with reliable statistics, most of the computation time of the coupled calculation is spent in running the Monte-Carlo calculation. However, using parallel processors it is possible to reduce significantly the computation time, and complete the coupled run in reasonable time. Hence, the coupled approach was developed for a multiprocessor environment. By means of Portable-Batch-System scripts, MCNP5 is run in parallel while SUBCHANFLOW is run consecutively in a single processor mode. The developed coupling scheme was applied to perform detailed 3D simulations of a BWR array and HCPWR fuel assembly.

2. Codes used in the coupled calculations

The Monte-Carlo code MCNP5 and the thermal-hydraulic sub-channel code SUBCHANFLOW are selected for these investigations. In addition, NJOY modules LEAPR, THERMR, ACER, and BROADR are used to process the nuclear data.

2.1. The thermal-hydraulic sub-channel code SUBCHANFLOW

For performing the sub-channel analysis, SUBCHANFLOW, a code developed at the KIT, was used (Imke, 2010), (Sanchez et al., 2010). It is based on the COBRA code family and is able to treat hexagonal and square bundle geometries with axially varying cell size. SUBCHANFLOW is written in FORTRAN 95 language in a fully modular way. Global data structure as well as fluid and material properties are stored in separate modules. The code solves mass, axial momentum, lateral momentum and energy conservation equations for vertical flow conditions. In contrast to all COBRA-versions, it is based on SI system of units. SUBCHANFLOW contains

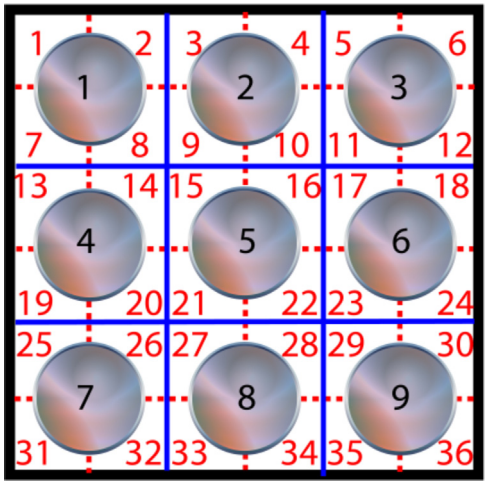

Fig. 1. Nodalization in SUBCHANFLOW and MCNP for the BWR array.

water, lead, helium, lead-bismuth and sodium as working fluid. Using thermal-hydraulic modeling based on 3 equations approach, SUBCHANFLOW can simulate a problem with 1156 sub-channels within two minutes. In contrast to COBRA-TF, SUBCHANFLOW can perform steady state calculations.

2.2. The neutronic code MCNP5 and the nuclear data processing code NJOY

MCNP5 simulates neutron transport in three dimensions using Monte-Carlo technique (Brown, 2005; MCNP, 2004). In the coupled run MCNP5 is used to generate the power profile, which is then transferred to SUBCHANFLOW. In order to read the power profile neutron tally (F7:n) and mesh tally (F4:n) are used. The NJOY99 module BROADR (NEA, 2006) was used to generate Doppler-Broadened continuous energy cross sections for subsequent use in the actual MCNP run. In addition to the BROADR module, the THERMR-LEAPR-ACER module sequence was used to prepare thermal scattering data at different temperatures.

3. MCNP5/SUBCHANFLOW coupling scheme

When coupling codes describing different physical phenomena, in particular neutronic and thermal-hydraulic phenomena, the spatial discretization of both domains has to be mapped to each other so that the exchange of information, in this case the thermal-hydraulic feedback parameters and the power profile, can be carried out in a consistent manner. In addition, the initialization run and the initial values for the feedback parameters and power distribution of the iteration loop are also important. Furthermore, a converged solution should be obtained after running reasonable number of coupled neutronic/thermal-hydraulic iterations.

3.1. The radial spatial mapping of neutronic and thermal-hydraulic domains

The ideal case is to have a bijective mapping between the axial and radial nodalizations of the two codes. This was the case for the investigations performed here. In order to transfer data between the codes, two PERL-scripts were developed for the automatic data interchange between the domains and for convergence handling. In Fig. 1, the SUBCHANFLOW discretization (sub-channels) is shown with dotted lines and the corresponding MCNP discretization (fuel cell universe) is shown with solid lines. The numbers in the fuel pin centres show the fuel pin numbering and the numbers located

inside the coolant show the sub-channel portions associated with each pin.

In order to read the axial power profile F4:n neutron mesh tally, together with MCNP5 tally multiplication card feature were used. Again the mesh tally should be chosen in coherence with the axial nodalization of the sub-channel code. Using mesh tally is only an approximation justified in the case of the BWR lattice due to its homogeneity. For the case of the HCPWR, fission heat deposition was tallied in each fuel cell. Special subroutine was written and included in the MCNP source. This subroutine extracts the accumulated tally data organizes it and prints three-dimensional power tables to be directly used by the thermal-hydraulics code. Reading and sorting the tally data with an external script, is not very effective and can be significant problem if complicated geometries are considered. It is important to emphasize that cell averaged values for the fuel temperature are supplied to MCNP. For the current study nine radial positions r_i were considered. At those radial positions nine values for the fuel temperature $T_{rad.i}$ were computed, and the following cell averaged value (1) was used in MCNP. Here r_9 is the outermost radius of the fuel cell, and the corresponding $T_{rad.9}$ is the pellet surface temperature.

$$T_{averaged} = \frac{1}{\pi r_9^2} \sum_{1}^{9} \pi T_{rad,i} (r_i^2 - r_{i-1}^2) \quad (1)$$

The moderator density and temperature were averaged using the sub channel area.

Each coupled calculation begins with a SUBCHANFLOW run assuming a cosine axial power profile and a flat radial pin power distribution. Following the previous work performed at the KIT (Sanchez and Al-Hamry, 2009), the variation of the node averaged fuel temperature is used for checking the convergence. The following criterion (2) is imposed on the fuel temperature, and is used as an estimate for the convergence,

$$\Delta T_{ij} = \left| \frac{T_{ij}^{last} - T_{ij}^{prev}}{T_{ij}^{last}} \right| < \varepsilon \quad (2)$$

where the index "*i*" is the pin number and "*j*" is the axial cell number. The indexes run over all pin cells in the problem. It should be taken into account that the tallies used to sample the power profile distribution have statistical uncertainties affecting the fuel temperature. This statistical uncertainty should be taken into account when choosing the convergence parameter ε. In particular, choosing very small ε, without taking into account the statistical uncertainty will result in convergence failure.

In Fig. 2 the scheme of the coupled system MCNP5/SUBCHANFLOW is shown.

In order to avoid long waiting times in the queue, the coupled calculation is performed by a single batch job.

It is worth to mention that this approach of coupling is flexible to treat variety of problem geometries providing the specific formalism, when input files for the calculation are prepared. This flexibility is made possible by using keyword markers and the powerful pattern matching capabilities of PERL language.

3.2. The Doppler broadening of nuclear cross sections

Nuclear cross sections depend on relative velocity in the centre of mass frame, temperature induced oscillations of the target atomic nuclei, inducing such changes result in Doppler Effect, being one of the most important phenomena in nuclear reactor safety. From the thermal-hydraulic calculation, different material temperatures are supplied. Hence the temperature effect on the corresponding nuclear cross sections should be considered. MCNP is capable of making corrections to the scattering cross section by

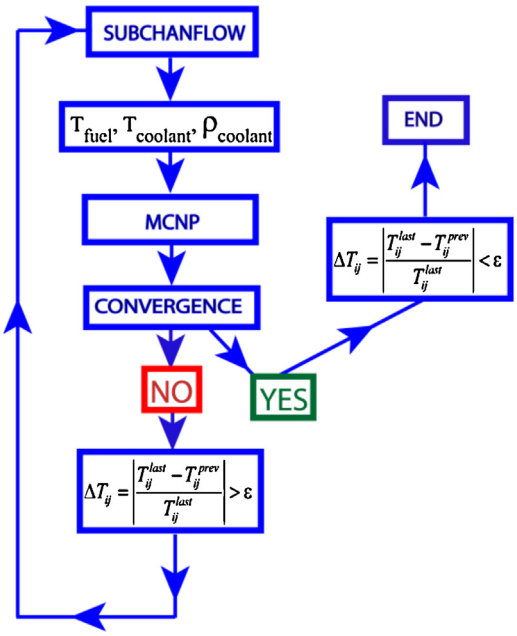

Fig. 2. Coupled MCNP5/SUNCHANFLOW system.

supplying the kinetic energy corresponding to the most probable velocity of the target nucleus via the TMP card (Watta et al., 2006; Brown, 2005). This is however, not enough to treat the full temperature dependence.

A possible solution to the Doppler broadening of the nuclear data is to adapt online nuclear data processing, by running the NJOY module BROADR at each iteration step as proposed in (Jouanne, 2010). However in practical terms this approach results in large CPU time running BROADR, and large memory demand to store the broadened data. In order to avoid this situation, another more practical approach was followed here. After initial run of the thermal-hydraulic code, intervals in which the fuel and the moderator temperature vary were determined. Later on, these intervals were divided into 50 K or 100 K increments. For the case of 50 K intervals BROADR was used to generated the necessary broadened cross sections based on JEFF.3.1.1 library. For the case of 100 K increments nuclear data based on JEFF 3.1 already available on the KIT computer cluster was used. BROADR was run by using automatic tool, enabling the preparation of cross sections based on user defined parameters. In the actual MCNP calculation, pseudo material mixing was used to correct for the temperature dependence of the nuclear data during the coupled calculation. Using this method pseudo material mixtures are assigned to each fuel/coolant cell. The two materials used in the mixture have temperatures, being the lower and the upper bound of the particular interval, in which the actual temperature obtained from SUBCHANFLOW is lying. For the atom fraction of the material obeying lower temperature we have (3).

$$f_{low} = \frac{\sqrt{T_{high}} - \sqrt{T_{actual}}}{\sqrt{T_{high}} - \sqrt{T_{low}}}, \quad (3)$$

for the higher temperature material in the mixture we have (4)

$$f_{high} = 1 - f_{low}. \quad (4)$$

By using the pseudo material mixing approach we obtain the following cross section mixture (5)

$$\Sigma_{pseudo}(T_{actual}) = f_{low} \Sigma_{low}(T_{low}) + f_{high} \Sigma_{high}(T_{high}) \quad (5)$$

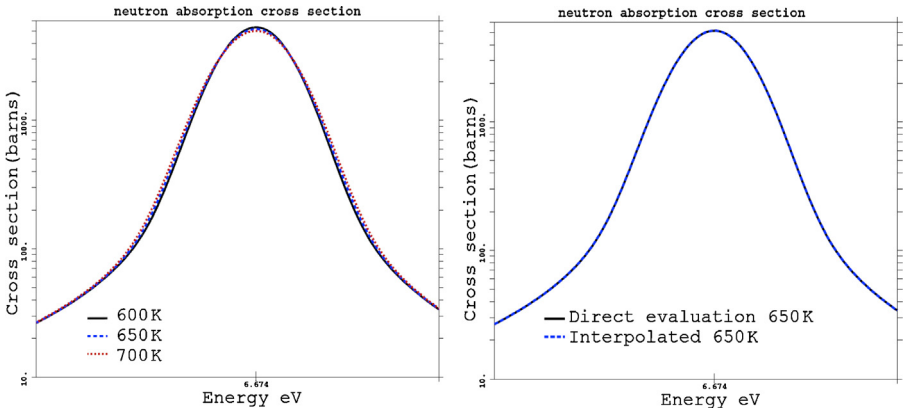

Fig. 3. Evaluations of the absorption cross section for three different temperatures (left) and comparison between NJOY-BROADR generated nuclear cross section and pseudo material mixing approach (right) for the 6.674 eV resonance of U^{238}.

It should be taken into account that pseudo material mixing is not interpolation in the classical sense. Using this method we rely on the stochastic nature of the neutronics code and there exists no nuclear data generated at some intermediate temperature. When the individual neutrons enter specific cell, they can interact with a certain nuclide at a given temperature with probability defined by its atomic fraction.

In order to illustrate this method, two simultaneously plotted cross sections for the main important resonance of U^{92}_{238} at 6.674 eV are shown in Fig. 3. One cross section is obtained via BROADR at temperature of 650 K and the other one is obtained as described by formula (5) by mixing 700 K and 600 K.

The consistency of both the linear and square root weighting was validated on a HCPWR fuel assembly loaded with MOX fuel. MOX fuel was used because the mixture of uranium and plutonium isotopes is expected to show larger sensitivity to thermal flux changes. Complete description of the fuel assembly geometry can be found in (Broeders, 1992) and in the last chapter of this paper. The fission source was sampled based on radial power profile distribution obtained via SCALE-NEWT. Based on this approach, it was possible to start the calculation with only 10 skipped cycles. In order to obtain good statistics, 350 active cycles with 350k (350,000) histories per cycle were used. Reflective boundary conditions were imposed on all bounding surfaces. The following test strategy was adopted: at the beginning nuclear data was produced, via NJOY-BROADR, at a temperature grid having 50 Kelvin intervals. Consequently few temperatures were selected and for these temperatures k_∞ values were computed. Later on, these temperatures were interpolated using their bracketing neighbors with either the linear or the square root weighted pseudo material mixing. The so obtained values for the multiplication factor are shown in Table 1. These tests resulted in good agreement between the direct and interpolated cases. Throughout the paper the standard deviation is given in pcm, where 1 pcm = 10^{-5}

Further proof for the validity of the pseudo material mixing methodology can be found in (van der Marck et al., 2005), where it was tested against benchmark results and experimental data.

Table 1
k_∞ computed with exact NJOY-BROADR processed data, and using the pseudo material mixing approach. The standard deviation is given in brackets.

Temperature (K)	NJOY-BROADR	Linear mixing	Square root mixing
1000	1.13999 (7 pcm)	1.13992 (6 pcm)	1.13990 (6 pcm)
1150	1.13534 (6 pcm)	1.13540 (6 pcm)	1.13540 (6 pcm)
1250	1.13243 (6 pcm)	1.13255 (6 pcm)	1.13242 (6 pcm)
1400	1.12845 (6 pcm)	1.12841 (6 pcm)	1.12846 (6 pcm)

3.3. Extension of the pseudo material mixing to the thermal scattering data

In order to treat the thermal scattering from bound scatterers MCNP utilizes additional thermal scattering data files, prepared by the LEAPR-THERMR-ACER modules sequence of NJOY. While the Doppler broadening module BROADR is capable of producing cross-section files at all desired temperatures, LEAPR requires frequency spectrum of the scattering nucleus $\rho(\omega)$ for each temperature in order to generate the scattering law $S(\alpha,\beta)$. For the current study the LEAPR input given in (Mattes, 2005) was used. In addition the THERMR module of NJOY was used to generate the point-wise thermal scattering cross-sections in PENDF format and the ACER module of NJOY was used to generate thermal scattering data for MCNP code in ACE format. Plot of $\rho(\omega)$ for the temperatures available is shown in the following Fig. 4

When performing coupled calculations, moderator temperatures may be significantly different from the temperatures, at which the thermal scattering data is available. If no action is taken the thermal scattering data will always be used inaccurately. The standard approach to correct for this effect is a simple extension of the pseudo material mixing approach. In the MCNP material card one can specify two materials and by changing the corresponding atom fractions temperature interpolation can be performed. However, this is not possible in the case of thermal scattering data. The material transformation card will always apply to one isotope of

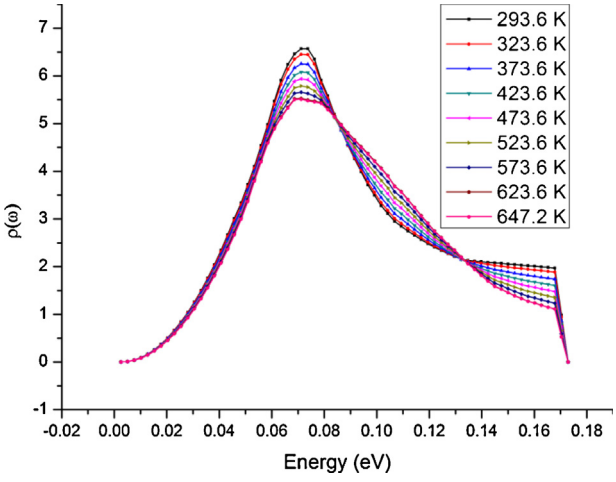

Fig. 4. Frequency spectrum of the scattering nucleus $\rho(\omega)$ for all the available temperatures.

```
m1        1004.97c  0.333333   $ H 523.6 K
          8016.97c  0.166667   $ O 523.6 K
          1006.99c  0.333333   $ H 623.6 K
          8016.99c  0.166667   $ O 623.6 K
mt1       lwal06.31t  lwal08.31t
```

Fig. 5. Illustration of the pseudo material thermal scattering mixing for 573.6 K.

hydrogen only. There exists a simple trick to overcome this obstacle. One defines pseudo isotopes of hydrogen (1004 1005 1007...) at specific temperatures, coinciding with the temperatures, at which the thermal scattering data is available. In coherence with this, the isotope index is changed correspondingly in the thermal scattering data files. From this point on, MCNP treats the modified data files for hydrogen as separate isotopes and it is possible to utilize more than one thermal scattering data file for hydrogen in water, within single material transformation card. Mixing is performed via the atom fractions as usual. For completeness a sample MCNP material card is shown in Fig. 5. In this example 1004.97c and 1006.99c are NJOY evaluations of hydrogen for 523.6 K and 623.6 K, where lwal06.31t and lwal08.31t are the corresponding thermal scattering data files produced by LEAPR-THERMR-ACER sequence. The temperature being interpolated is 573.6 K.

This approach was tested on a PWR fuel assembly loaded with UOX fuel, and reflective axial and radial boundary conditions. The following comparison procedure was adopted: At the beginning k_∞ values were obtained, using LEAPR-THERMR-ACER sequence of NJOY generated thermal scattering data. Later on, two specific temperatures, at which exact data was available, were interpolated using the above-described weighting procedure. A comparison was carried out between the direct evaluated and linear or square root mixed data. In order to obtain good statistics, 300 active cycles with 350k particles per cycle were run. The initial fission source was sampled based on SCALE-NEWT radial pin power distribution, allowing reduction of the initial skipped cycles to ten. The results together with the problem geometry are shown in Fig. 6 On the basis of this test it can be concluded that the pseudo material mixing strategy produces consistent results and it can be further used to interpolate the thermal scattering data.

It should be taken into account that 573.6 K was interpolated using the data available at 523.6 K and 623.6 K and 623.6 using the data available at 573.6 K and 647.2 K. In the actual coupled calculation, as it can be deduced from the available temperatures on the $\rho(\omega)$ plot, the interpolation temperature intervals are reduced and even better results are obtained.

3.4. Convergence of the iterative coupled solution

Due to nonlinear nature of the coupled physics, a large number of iteration may be needed to get a converged solution. Based on the previous work, the implementation of a relaxation method was done to speed-up the convergence behavior of the coupled system (Sanchez and Al-Hamry, 2009). Since the local fuel temperature shows the largest oscillations during the coupled runs, it was selected to be the convergence parameter (Sanchez and Al-Hamry, 2009). Plotting different cycles of a coupled run, it was observed that the axial power profile performs damped oscillations around the final converged value, resulting in oscillations of the node averaged fuel temperature. In this approach, the actual thermal-hydraulic parameters will be mixed with the ones of the previous step according to the following relation. Particular example for the cell averaged fuel temperature is the following formula (6).

$$T_{fuel,i}^{weighted} = (1-\omega)T_{fuel,i-1} + \omega(T_{fuel,i}^{actual}) \quad (6)$$

Here ω is a parameter determined from parametric study. In (Sanchez and Al-Hamry, 2009) it was found that a value of $\omega = 0.5$ leads to optimal results for the PWR case. For the BWR case stronger under-relaxation was needed using $\omega = 0.6$. The remaining thermal-hydraulic parameters were also mixed in the same manner as the fuel temperature. Using this approach computation time and the number of iterations were significantly reduced.

The damping of the axial power profile oscillations, as a consequence of the relaxation scheme, is shown in Fig. 7. Coupled iteration runs 7 and 8 from two different calculations are presented. If no relaxation is applied, as evident from the graph the solution is still divergent after running 8 coupled iterations. Using the relaxation method the number of coupled cycles needed to get converged results could be reduced from 15 to 8.

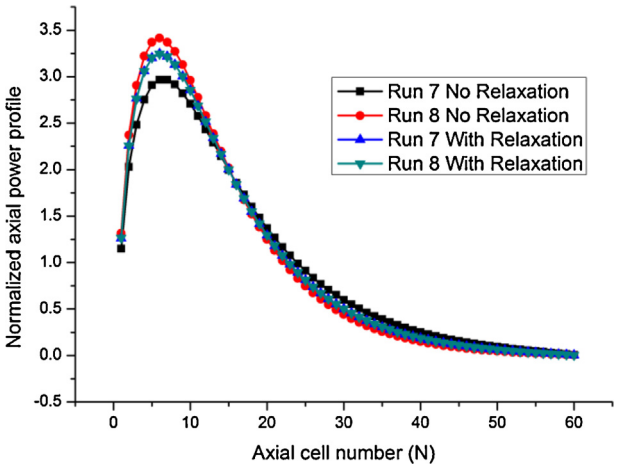

Fig. 7. Axial power profile shape after running eight coupled iterations showing the effect of the relaxation scheme, $\omega = 0.6\%$.

3.5. Refinement of the nuclear data temperature grid

Another important aspect affecting the coupled calculations is the values at which the nuclear data is processed via NJOY. In the case of the thermal scattering data the possible values are fixed. In

Temperature	Exact value	Pseudo material (sqrt)	Pseudo-material(linear)
573.6 K	1.39430(6pcm)	1.39443 (6pcm)	1.39436(6pcm)
623.6 K	1.39350(6pcm)	1.39353 (5pcm)	1.39343(5pcm)

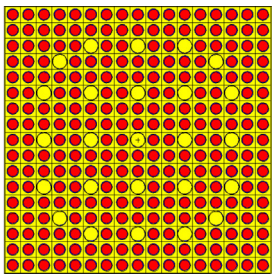

Fig. 6. $S(\alpha,\beta)$ interpolation using pseudo material mixing. The standard deviation of k_∞ is given in brackets. The problem geometry is shown on the right hands side.

the case of the continuous nuclear data the grid can be made either finer or coarser. In order to investigate this effect, two coupled runs were performed. One coupled run was done with nuclear data prepared at 100 K grid and another one with nuclear data prepared at 50 K grid. For the 100 K grid JEFF 3.1 based NJOY processed data already available at the KIT was used. For the 50 K grid case new data set was prepared using JEFF 3.1.1. Identical thermal scattering data was used in both the cases.

As expected the pseudo material mixing provided better results for the 50 K grid, and the convergence was met earlier. Results of the comparative runs are shown in Table 2.

Both the k_∞ and the axial power profiles predicted by the two runs are very similar. The faster convergence observed for the 50 K increments case can be attributed to the fact, that the finer grid gives better results when pseudo material mixing is done. No difference outside the statistical uncertainty limit was observed in the case of the axial power profile.

3.6. Monte-Carlo tallying and fission source convergence

Monte Carlo codes use the source iteration method to estimate the eigenvalues and eigenvectors of the stationary transport operator. In operator notation the transport equation is defined as:

$$\varphi = \frac{1}{k}\mathbf{L}\varphi \tag{7}$$

This means that we generate successive states by applying the transport operator $\mathbf{L}$ over a number of criticality cycles:

$$\varphi^n = \prod_{i=0}^{n-1}\frac{1}{k^i}\mathbf{L}^n\varphi^{(0)} \tag{8}$$

The transport operator $\mathbf{L}$ has discrete spectrum and therefore, satisfies eigenvalue equations of the type:

$$\varphi^n = \frac{1}{k^n}\mathbf{L}^n\varphi^n \tag{9}$$

This allows us to write the following expansions in terms of the eigenfunctions:

$$\varphi^{(0)} = \sum_l \alpha_l\varphi^l\left(\frac{1}{k^1}\mathbf{L}\right)^n\varphi^{(0)} = \alpha_1\varphi^1 + \alpha_2\left(\frac{k^2}{k^1}\right)^n\varphi^2 + \sum_{l>2}a_l\left(\frac{k^l}{k^1}\right)^n\varphi^l \tag{10}$$

From (10) one sees that the convergence is determined by the ratio $\frac{k^2}{k^1}$, which is the dominance ratio of the system. If this ratio is close to unity, the system is called to have high dominance ratio.

It is well know that the multiplication factor and the source have different convergence behavior in Monte-Carlo simulations. The multiplication factor being an integral quantity converges much faster than the fission source spatial distribution. Performing tallying before the source has converged will result in erroneous tally estimates, and will jeopardize the calculation. In MCNP5 it is possible to check the convergence using the Shannon entropy and doing so to ensure that tallying is done after the fission source has converged. In practice, to speed up the source convergence, an initial source distribution is calculated by MCNP using thermal-hydraulic feedback generated with a homogeneous radial and cosine axial power profiles. This source distribution is used further and updated during the subsequent coupled iterations. Due to the significant changes of the thermal-hydraulic during the initial coupled runs, the source is generated under iteration-to-iteration varying conditions. In order to be consistent, the skipped cycles are set to conservative initial value, for instance 50 for the HCPWR, and are reduced in the consequent iterations. The values of the Shannon entropy normalized with respect to the mean value for the active criticality cycles are plotted in Fig. 9. Two cases are shown; one corresponds to the HCPWR assembly and the other one to the BWR array. Both of these calculations were started with source defined via SDEF card. The fission source SRC files generated during these initializing runs were used for the subsequent calculations. Cosine axial and flat radial power profiles were assumed in order to sample the fission source probability in both cases. Thermal-hydraulic boundary conditions were generated by SUBCHANFLOW using flat radial and cosine axial power profiles. It is evident from Shannon entropy plots that the fission source has converged over the active criticality cycles therefore it can be concluded that reasonable estimate was done for the number of the initial skipped cycles. In Table 3 the main parameters of the stand-alone MCNP5 simulations for a HCPWR and BWR 3×3 pin cluster are summarized.

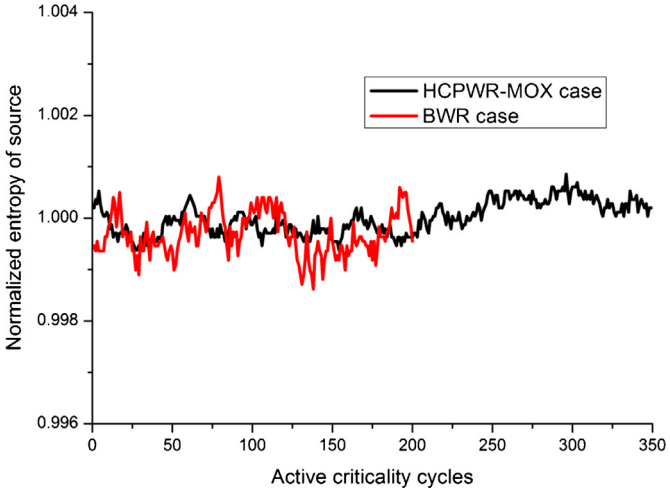

Fig. 8. Plots of source entropy versus number of criticality cycles for the BWR lattice and the HCPWR cases.

The standalone calculations were used in order to judge upon the expected tally variances and to determine the optimum number of initial skipped criticality cycles.

It is evident from Fig. 8 that Shannon entropy is converged over the active cycles. Besides the standard method of using source distribution obtained from previous MCNP run, another method was tested. Using SDEF card and power profile distribution obtained from deterministic code it is possible to sample the fission source. This strategy was illustrated for the 2D problems discussed in Chapters 3.1 and 3.2. Currently, a coupling between the SP_3 code NEM and SUBCHANFLOW is being developed. The converged values for the power profile distributions from NEM-SUBCHANFLOW are to be used for sampling the fission source. The advantage of this method is that the power profile can be obtained for the specific iteration by supplying the same thermal-hydraulic boundary conditions to NEM. In theory, it is possible to reduce the initial skipped cycles to zero. To provide maximum coherence between NEM and MCNP, homogenized cross sections are to be prepared by SERPENT Monte-Carlo code (SERPRENT, 2011), based on the continuous nuclear data used by MCNP. In addition, the converged values for the thermal-hydraulic feedback parameters from NEM-SUBCHANFLOW coupled run will be used as initial conditions for the MCNP-SUBCHANFLOW calculation. In this manner a significant acceleration of the coupled MCNP-SUBCHANFLOW scheme is expected. This research follows the methodology explained in (Puente-Espel et al., 2010).

Table 2
Comparison between the coupled runs with cross sections prepared at 100 K and 50 K increments.

Case	Cycles skipped	Cycles total	Histories per cycle	k_∞	Coupled runs
100 K (JEFF 3.1)	10	160	200k	1.10298 (10pcm)	11
50 K (JEFF3.1.1)	10	160	200k	1.10341 (11pcm)	8

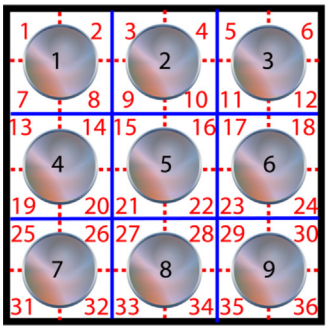

Total length	3.71 m
Number of axial nodes	60
Inlet coolant temperature	551.93 °C
Coolant mass flow rate	1.1205 kg/s
Total power	0.551 MW
Exit pressure	7.0 MPa
Pin radius	0.5375 cm
Pellet radius	0.45555 cm

Fig. 9. BWR 3 × 3 lattice geometry parameters and thermal-hydraulic boundary conditions.

Table 3
Summary of the standalone calculations.

FA Type	Axial nodes/pins	Histories/active cycles	Skipped cycles	Processors/time standalone run	k_∞
HCPWR (MOX)	20/271	400k/350	50	96/5.5 h	1.13387 (6)
HCPWR (UOX)	20/271	400k/350	50	96/5 h	1.23684 (6)
BWR (UOX)	60/9	200k/200	30	16/25 min	1.25221 (7)

4. Application of the coupled scheme to SPECIFIC problems

The developed MC/TH coupling scheme will be applied for the pin-by pin simulation of both a BWR 3 × 3 pin cluster and of a large hexagonal fuel assembly of an innovative reactor concept, the High Conversion PWR (HCPWR). A short description of the problem geometry as well as the main results will be presented hereafter.

4.1. BWR 3 × 3 pin cluster problem

The BWR 3 × 3 pin cluster consists of nine fuel rods with the dimensions and operational conditions as shown in Fig. 9.

Due to the large coolant density gradient, 60 axial nodes were considered in both MCNP and SUBCHANFLOW (Imke, 2010), (Sanchez et al., 2010). Considering that many axial nodes is advisory, doing the opposite will give very crude description of the boiling occurring in the 3 × 3 lattice, and shall result in supplying coolant densities averaged over large moderator cells to the MCNP code.

In the radial direction, the MCNP5 model uses reflective boundary conditions while axially vacuum conditions are implemented. Giving vacuum boundary conditions on the axial planes is necessary in order to compute realistic axial power profile. In SUBCHANLOW sixteen sub-channels are considered. In order to compute the cell averaged fuel temperature 9 radial nodes were considered in the fuel. The thermal-hydraulic conditions specified in Fig. 9 are used for the sub-channel code model. For the coupled simulations the MCNP5 parameters given in Table 4 were used. The coupled

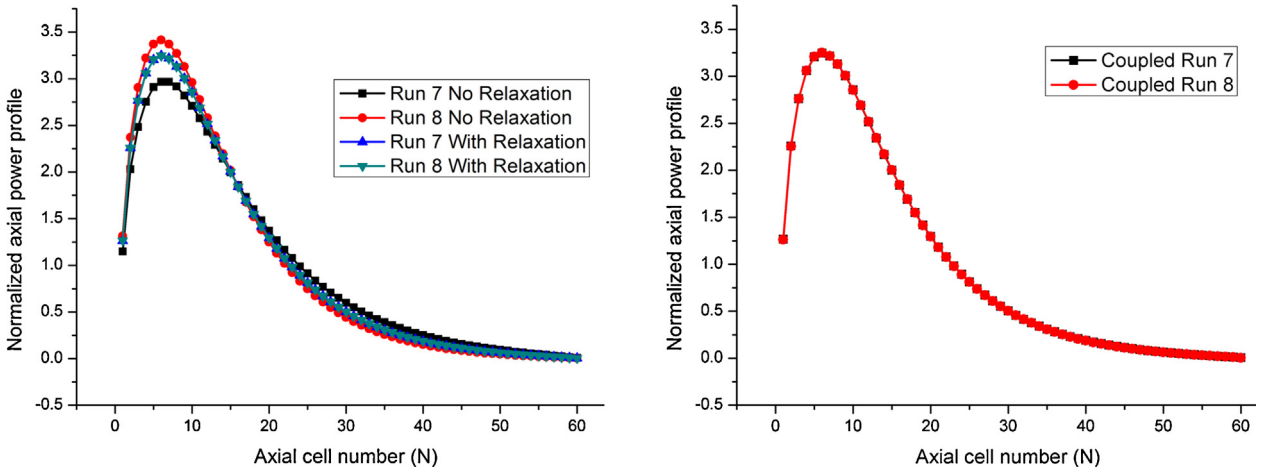

Fig. 10. Axial power profile evolution (left) and the final iterations where convergence is satisfied (right).

Table 4
Radial power profile of the BWR lattice and calculation run summary.

Pin7 = 1.0000	Pin8 = 0.9998	Pin9 = 1.0001
Pin4 = 1.0002	Pin5 = 0.9999	Pin6 = 1.0004
Pin1 = 1.0000	Pin2 = 0.9998	Pin3 = 0.9998

Parameter	k_∞	Standard deviation	Histories/Cycles	Skipped cycles	Processors/Cycle run time	Parallel run
Value	1.10341	11 pcm	200k/200	30	60/25 min	8

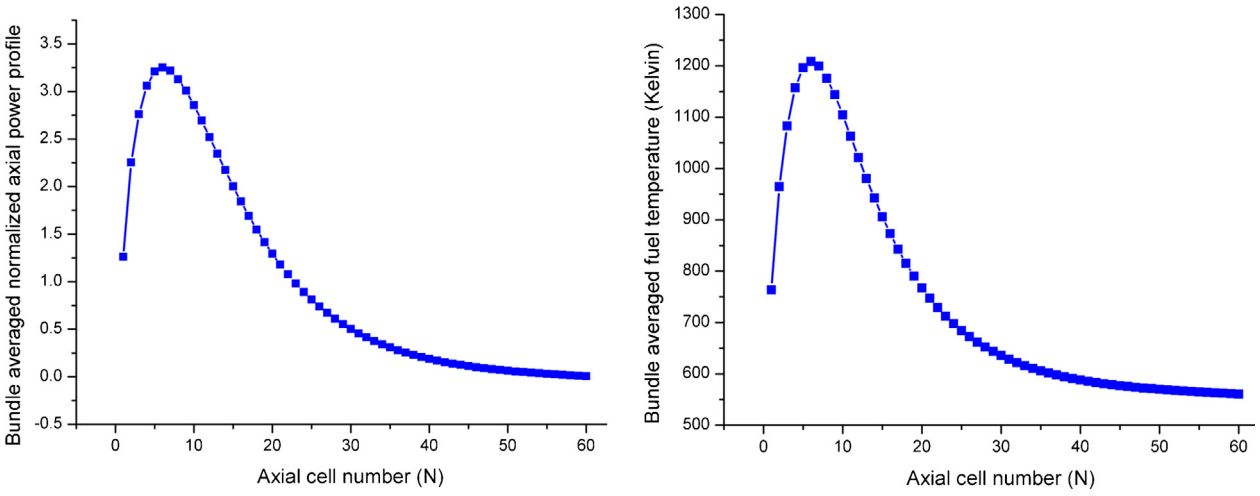

Fig. 11. Axial power profile of the 3 × 3 BWR lattice and node averaged fuel temperature distribution.

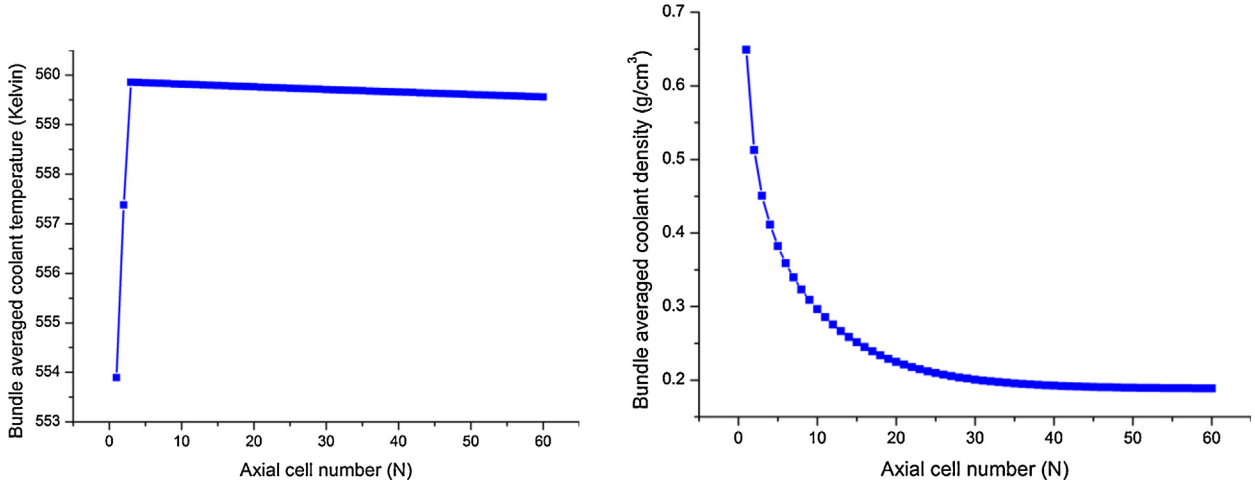

Fig. 12. Coolant temperature and density distributions along the axial height of the 3 × 3 BWR lattice.

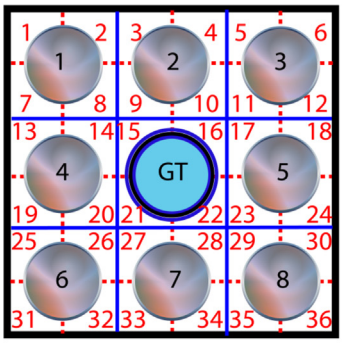

Total length	3.9 m
Number of axial nodes	10
Inlet coolant temperature	563.15 K
Coolant mass flow rate	2.58 kg/s
Total power	0.532 MW
Exit pressure	15.8 MPa
Pin radius	0.475 cm
Pellet radius	0.411 cm
Guide tube radius	0.6175 cm

Fig. 13. PWR 3 × 3 lattice and thermal-hydraulic boundary conditions.

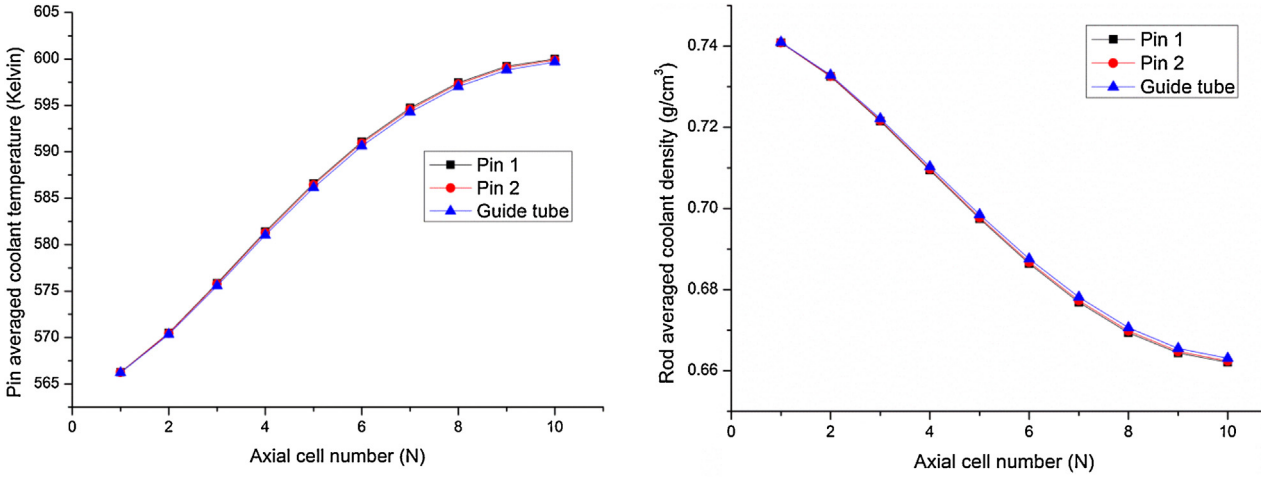

Fig. 14. Coolant temperature and coolant density axial distributions for selected pins of the PWR fuel assembly.

solutions converged after eight iterations. For the particular case, the convergence parameter $\varepsilon = 0.5\%$ was chosen. It took 25 min in order to run one coupled step, where most of the time was spent in running the MCNP code, in contrast to the fast running SUBCHANFLOW code, which takes about 5 s computation time.

In Fig. 10 the evolution of the axial power profile over the coupled iterations together with the last two iterations before convergence was met is shown. In Fig. 11, the bundle averaged axial power profile and the bundle averaged fuel temperatures are shown. As expected, the highest fuel temperature corresponds to the highest axial power. Both are located in the lower part of the fuel rod, where the coolant is colder and hence denser compared with the upper part.

The axial bundle averaged coolant temperature distribution and the coolant density are shown in Fig. 12. The large density decrease is typical in BWR cores. It can be clearly seen that due to the large power peak in the bottom, fluid reaches boiling temperature already in the lower part of the lattice leading to the shift in the axial power. From these calculations it can be determined that the coolant density feedback has the biggest impact on the power profile.

Finally, the predicted radial power profile is given in Table 4 together with the computed value of k_∞. As expected, due to lack of heterogeneities in the lattice the radial profile is practically flat.

4.2. PWR 3 × 3 pin cluster problem

In order to study heterogeneous geometries the coupled system was extended adding additional subroutine to MCNP. With this subroutine it was possible to tally fission heat deposition in all pins of interest and to print the tally results in SUBCHANFLOW readable format. In contrast to the BWR lattice it is no longer possible to read the axial power profile by mesh tally. Using the new methodology it was possible to define individual power profile for all pins in the problem. The new methodology was tested on 3 × 3 PWR array containing a single guide tube. The same strategy was applied later on to the HCPWR problem. Operating conditions and geometry representation are given in Fig. 13 In the case of the PWR there exists no large axial density gradient as in the case of the BWR and therefore, only 10 axial nodes where considered. The relaxation parameter $\omega = 0.5$ and convergence criterion $\varepsilon = 0.2\%$ were chosen.

The coupled calculation converged within 6 coupled runs. Results for the radial power profile distribution and coupled run statistics are shown in Table 5. As expected the pins closer to the guide tube had larger relative power. This can be explained with the presence of large coolant volume in the vicinity of those pins. As expected due to the lack of fission heat deposition in the guide tube, the coolant density is larger and the coolant temperature is smaller than for those sub-channels closest to the guide tube.

Plot of the sub-channel averaged values for two selected pin and the guide tube are shown in Fig. 14

Due to the lack of large density gradient the power profile, and hence the fuel temperature axial distributions had shapes close to the cosine distribution. A plot of the axial fuel temperature distribution for two selected pins at the last two coupled iterations is shown in Fig. 15

4.3. Application of coupled calculation MCNP-SCF scheme to the HCPWR fuel assembly

The third problem investigated is an innovative HCPWR fuel assembly composed of 247 pins and 24 guide tubes. The same mapping scheme as the one used for the PWR fuel assemblies is used here. The operational conditions of the HCPWR together with the geometry are given in Fig. 16. The data is taken from KfK report 5072 (Broeders, 1992). This is the same geometry input as the one used for testing the pseudo material mixing, the difference is that also the axial dimension is considered.

The HCPWR fuel assembly is characterized by a tight triangular lattice, where the neutron moderation was reduced aiming to

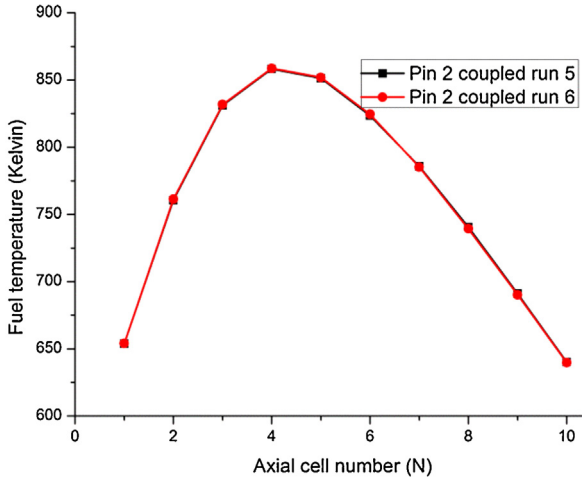

Fig. 15. Fuel temperature axial distribution for the last two coupled runs.

Table 5
Radial power profile of the PWR lattice and calculation run summary.

Pin6 = 1.1081	Pin7 = 1.1418	Pin8 = 1.1080
Pin4 = 1.1421	Guide Tube	Pin5 = 1.1420
Pin1 = 1.1081	Pin2 = 1.1420	Pin3 = 1.1079

Parameter	k_∞	Standard deviation	Histories/Cycles	Skipped cycles	Processors/Cycle run time	Parallel run
Value	1.32434	8 pcm	200k/200	30	60/18 min	6

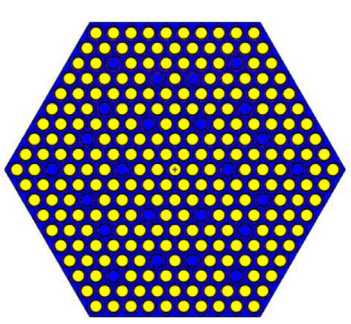

Total power	10.89 MW
Fuel assembly length	350 cm
Fuel pellet radius	0.4025 cm
Clad inner radius	0.411 cm
Pin radius	0.475 cm
Guide tube outer radius	0.475 cm
Guide tube inner radius	0.411 cm
Exit pressure	15.83e6 Pa
Inlet coolant flow rate	52.7 kg/s
Inlet coolant temperature	563.35 K

Fig. 16. High conversion PWR fuel assembly geometry and operating conditions.

Table 6
Number of nodes where ΔT_{ij} satisfies certain value of ε, the numbers given after the slash represent the percent form total.

ε	Run 8	Run 9	Run 10	Run 11	Run 12	Run 13	Run 14	Run 15
$\varepsilon < 2.0$	5415/99.9	5420/100	5415/99.9	5420/100	5420/100	5420/100	5420/100	5420/100
$\varepsilon < 1.5$	5174/95.5	5341/98.5	5282/97.5	5420/100	5420/100	5420/100	5420/100	5420/100
$\varepsilon < 1.0$	3928/72.5	4639/85.6	4316/79.6	5396/99.6	5397/99.6	5415/99.9	5219/96.3	5418/99.96
$\varepsilon < 0.5$	2303/42.5	3018/55.7	2422/44.7	4705/86.8	4705/86.8	4969/91.7	3516/64.9	4972/91.7
$\varepsilon < 0.25$	1348/24.9	1996/36.8	1478/27.3	3179/58.7	3183/58.7	3641/67.2	2105/38.8	3460/63.8

increase the conversion ratio. The HCPWR operates on MOX fuel with 14.67 wt% plutonium content. Additional test example was designed with MOX changed to UOX. For this geometry type 20 axial nodes in the fuel and moderator were defined. Due to the large number of tally cells (4940 fuel cells and additional 480 cells for the guide tubes) obtaining tallies with reasonable statistical uncertainty posed significant challenge and required large number particle histories. It should be taken into account that there is no fission heat deposition in the guide tubes and no tallying is done there. The number of histories per cycle was 400k and the total number of active cycles was 550. With this choice of KCODE parameters it was possible to obtain a maximum tally statistical uncertainty of 1.5% for the MOX case and 1.1% for the UOX case. The convergence parameter ε values were set to 1.6% and 1.2% correspondingly.

Regardless of the large number of cells and sub-channels defined in the MCNP/SUBCHANFLOW problem, the coupled calculation showed steady convergence behavior and needed 11 and 9 iteration runs, for the UOX and MOX cases correspondingly, until convergence criterion was met.

The strong correlation between the tally uncertainties and the convergence parameter is illustrated in Table 6 and Table 7. There can be seen a set of convergence parameter values and the number of nodes with ΔT_{ij} satisfying these values, over the course of few coupled iterations. For the UOX case the maximum tally uncertainty was ~1.1% and for the MOX case ~1.5%. As can be seen from these tables, in the limit of ε value reaching 1.1% and 1.5% correspondingly, it starts to show oscillatory behavior due to the statistical uncertainties, and reaching any finer convergence state is not possible. The finer convergence criterion in the UOX case explains also the larger number of cycles needed before convergence. In summary the maximum values of the tally uncertainties can be understood as an infimum of the ε values set. It should be noted that the coupled run was continued past the converged iteration to investigate the ε behavior. If one wishes to reduce the ε value, the statistical uncertainty of the tally estimates should be improved by simulating larger number of particle histories.

The computed axial power profile for two selected pins (MOX case) is shown in figure Fig. 17 along with the radial pin power distribution.

The computed axial power profile for two selected pins (UOX case) is shown in figure Fig. 18 along with the radial pin power distribution.

The power distributions are similar in nature to the ordinary PWR case. The lack of large density gradient resulted in power profiles similar to the cosine distribution. Similarly the pins located near large coolant volumes i.e. guide tubes and the assembly

Table 7
Number of nodes where ΔT_{ij} satisfies certain value of ε, the red numbers represent the percent from the total number of cells. MOX loading case.

ε	Run 7	Run 8	Run 9	Run 10	Run 11	Run 12	Run 13	Run 14
$\varepsilon < 2.0$	5420/100	5399/99.6	5420/100	5420/100	5420/100	5420/100	5420/100	5420/100
$\varepsilon < 1.5$	5420/100	4607/85	5420/100	5420/100	5418/99.9	4960/91.5	5420/100	5420/100
$\varepsilon < 1.0$	5292/97.6	2516/46.4	5420/100	5417/99.9	5129/94.6	3247/59.9	5385/99.3	5420/100
$\varepsilon < 0.5$	4041/74.6	1416/26.1	5238/96.6	4990/92.1	2638/48.7	1691/31.2	4591/84.7	5195/95.8
$\varepsilon < 0.25$	2315/42.7	851/15.7	4125/76.1	3695/68.2	1388/25.6	1041/19.2	3180/58.6	4004/73.9

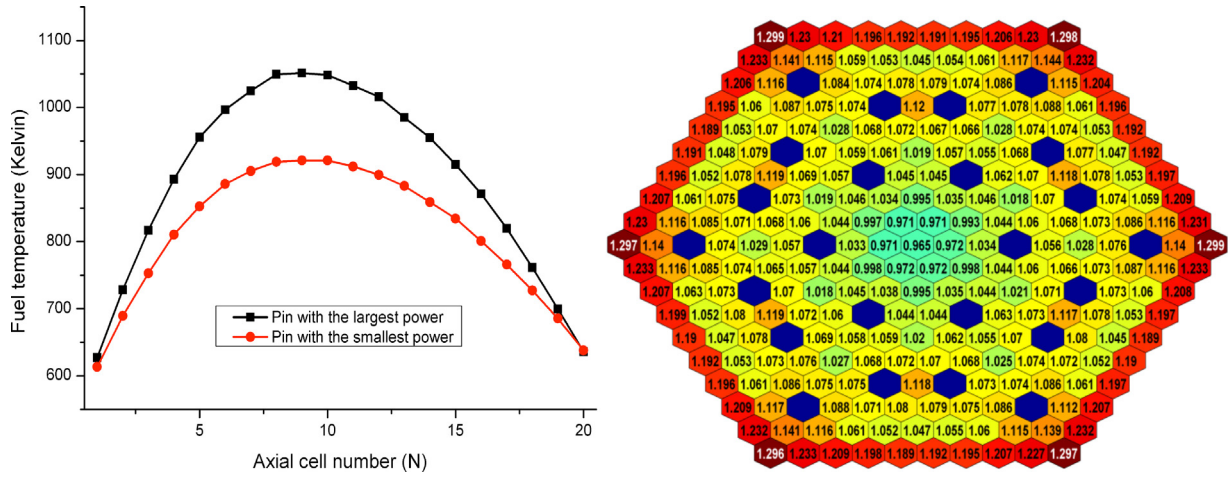

Fig. 17. High conversion PWR Fuel assembly axial power profile for selected pins and radial pin power profile distribution (MOX).

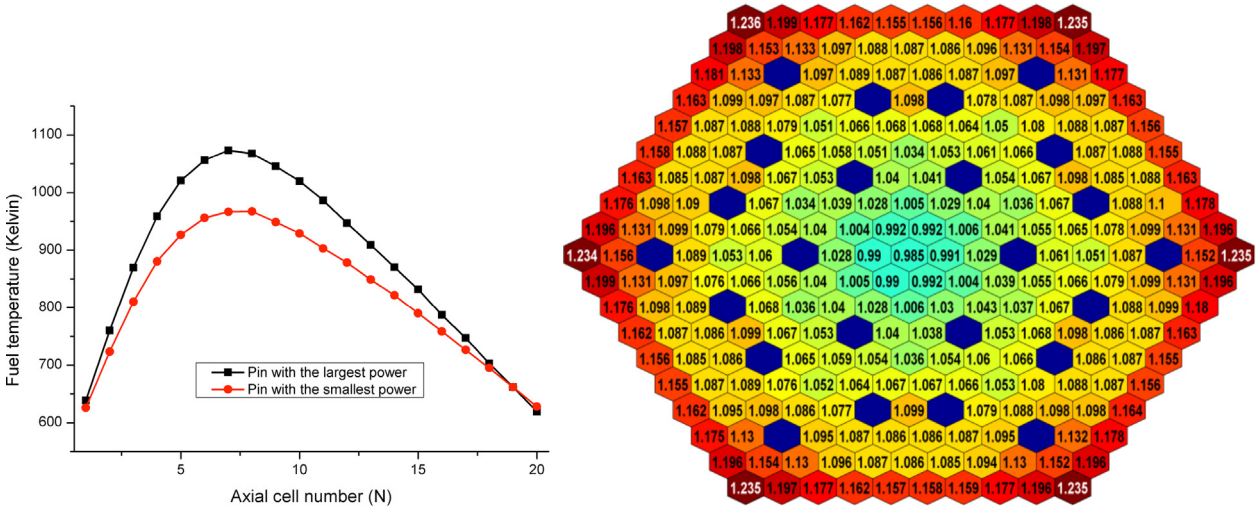

Fig. 18. High conversion PWR Fuel assembly axial power profile for selected pins and radial pin power profile distribution (UOX).

periphery had larger power output. In both cases the power profile distribution has azimuthal symmetry, and the pins with the maximal power are located in the six corners of the assembly. The pin with the smallest power for both the cases is located in the assembly center.

5. Conclusions

In this paper the coupled code system MCNP-SUBCHANFLOW was presented. It was shown that converged solutions can be obtained within reasonable number of iteration loops. The pseudo material mixing methodologies were used to correct for the temperature dependence of both continuous energy and thermal scattering data. In both cases, good agreement was found with respect to the reference values. Although promising results were obtained, additional improvements of the coupling strategy is needed. Currently at the KIT a subroutine, capable of direct interpolation of the thermal scattering data files produced by the LEAPR-THERMR-ACER sequence, is being tested.

Further improvements are currently being developed in order to speed up the coupled calculation. One proposal is the utilization of adaptive under-relaxation scheme. In this scheme the relaxation parameter and the number of histories are adapted over the course of the coupled calculation. Current tests of this scheme gave promising results and resulted in significant speedup. Another proposal is to use deterministic coupled system NEM-SUBCHANFLOW in order to provide realistic initial conditions close to the converged values and by doing so avoid starting the calculation with flat or cosine power distributions. This approach is also expected to reduce the number of skipped cycles.

Acknowledgements

The authors gratefully acknowledge the support of the Nuclear Safety Program of the Karlsruhe Institute of Technology.

References

Broeders, C.H.M. (1992) Entwicklungsarbeiten für die neutronenphysikalische Auslegung von Fortschrittlichen Druckwasserreaktoren (FDWR) mit komplexen Dreiecksgittern in hexagonalen Brennelementen. KfK 5072.

Brown, F. (2005) Fundamentals of Monte Carlo Particle Transport LA-UR-05—4983. Los Alamos National Laboratory. http://mcnp-green.lanl.gov/publication/pdf/LA-UR-05-4983_Monte_Carlo_Lectures.pdf

Hoogenboom, E., Diop, Ch., Ivanov, A., Sanchez, V., 2011. Development of coupling methodologies for TRIPOLI and FLICA in the frame of NURISP Project. In: The 2011 International Conference on Mathematics and Computational Methods Applied to Nuclear Science and Engineering (M&C 2011), Rio de Janeiro, RJ, Brazil, May 8–12.

Imke, U., 2010. Input Instructions for SUBCHANFLOW 1.6, KIT. Karlsruhe, Germany.

Jouanne, C., Trama, J. (2010) Linux Binary of TRIPOLI-4 capable of producing point cross-sections at various temperatures. NURISP Deliverable D.1.1.1.

Mattes, M. Keinert, J. (2005) Thermal neutron scattering data for the moderator materials H_2O, D_2O and ZrHx in ENDF-6 Format and as ACE Library for MCNP(X) Codes. IAEA Nuclear Data Section, Wagramer Strasse 5, A 1400 Vienna April 2005, INDC(NDS)-0470.

MCNP (2004) – A General Monte Carlo N-Particle Transport Code. Version 5. Los Alamos National Laboratory.

NEA/NSC/DOC (2006) 18, Processing of the JEFF-3.1 Cross Section Library into Continuous Energy Monte Carlo Radiation Transport and Criticality Data Library.

Puente Espel, F., Avramova, M., Ivanov, K., Misu, St., 2009. High accuracy modeling for advance nuclear reactor core designs using Monte Carlo Based coupled calculations. In: Invited Paper for M&C 2009. Saratoga Springs, New York, May 3–7.

Puente-Espel, F., Avramova, M., Ivanov, K., 2010. New developments of the MCNP/CTF/NEM/NJOY Code system-Monte Carlo based coupled code for high accuracy modeling. In: Proceedings of Advances in Reactor Physics to Power the Nuclear Renaissance (PHYSOR), Pittsburgh, Pennsylvania, USA, May 9–14.

Sanchez, V., Al-Hamry, A., 2009. Development of a coupling scheme between MCNP and COBRA-TF for the prediction of the pin power of a PWR fuel assembly. In: Proceedings of International Conference on Mathematics, Computational Methods & Reactor Physics (M&C 2009), New York, USA.

Sanchez, V., Imke, U., Ivanov, A., Gomez, R., 2010. SUBCHANFLOW: a thermal-hydraulic sub-channel program to analyse fuel rod bundles and reactor cores. In: 17th Pacific Basin Nuclear Conference, Cancún, México, October 24–30.

Sánchez, V., Al-Hamry, A., Broeders, C.H.M., 2008. Development and qualification of the coupled code system COBRA-TF/THREEDANT for the pin-by-pin power calculation. In: Proceedings of ICAPP '08, Anaheim, CA USA, June 8–12, Paper 8269.

PSG2/SERPENT (2011) Monte Carlo Reactor Physics Burnup Calculation Code. http://montecarlo.vtt.fi

Tippayakul, C., Avramova, M., Puente Espel, F., Ivanov, K., 2007. Investigations on Monte Carlo based coupled core calculations. In: Proceedings of ICAPP 2007, Nice, France, May 13–18, Paper 7134.

van der Marck, S., Meulekamp, R., Hogenbirk, A., 2005. New temperature interpolation in MCNP. In: Proceedings of M&C 2005 Conference, Avignon, France.

Watta, C., Schulenburg, T., Cheng, X., 2006. Coupling of MCNP with a sub-channel code for analysis of a HPLWR fuel assembly. FZKA7233. FZK, Karlsruhe Germany.